Sources of error within stable isotope and carbonate dissolution measurements of early Paleocene hyperthermals

Matt Ramlow

Geology and Geophysics, Class of 2011

April 27th 2011

Advisor: Mark Pagani, Geology and Geophysics

Second Reader: Hagit Affek, Geology and Geophysics

A Senior Thesis presented to the faculty of the Department of Geology and Geophysics, Yale University, in partial fulfillment of the Bachelor's Degree.

Abstract

During the Paleocene (65.5-55.8 Ma) and continuing on through the early Eocene (55.8-33.9 Ma) the Earth experienced numerous short-lived, extreme warming events called hyperthermals. Hyperthermals are marked by negative carbon isotope excursions indicating the addition of isotopically light carbon into the exchangeable reservoir. In addition these periods contain widespread carbonate dissolution possibly caused by massive inputs of new carbon decreasing the carbonate saturation state of the ocean. Evidence suggests that the major Paleocene and Eocene hyperthermal events were not random occurrences but part of a continuous series of similar, but smaller hyperthermal events. Spectral analysis studies of hyperthermals indicate they may be triggered by changes in isolation due to Milankovitch forcing. Recent studies have found a similar series of hyperthermal event occurring in the early Paleocene and this research seeks to reveal further evidence and analyze the periodicity of early Paleocene hyperthermals to better understand the Milankovitch forcing that may trigger these rapid warming events. This study sought to expand high resolution sampling of the Bottaccione section in central Italy, continuing past the documented DanC2 hyperthermal event, and collect samples from the Forada section in northern Italy. Stable carbon isotopes and carbonate dissolution were measured to identify hyperthermal events. This study would have performed spectral analysis to detect statistically significant periodicity between events but the dataset was determined to be unreliable. This study found that the stable isotope measurements contained levels of variance at best of ±0.32‰ $\delta^{13}C$, and the carbonate dissolution measurements contained a variance of at best ±16.5% $CaCO_3$. The uncertainties in the data outweigh the statistically significant variability between hyperthermal events (±1‰ $\delta^{13}C$ and ±15% $CaCO_3$) and background variance (±0.25‰ $\delta^{13}C$ and ±5% $CaCO_3$). The variance within the data set was found to be a result of imprecision within the mass spectrometer, as determined by variance within known standards, and not necessarily the natural variability from the Bottaccione or Forada section. This study analyzes sources of error that may occur within stable isotope and carbonate dissolution measurements and recommends further study of the Bottaccione and Forada sections to detect and analyze the evolution of early Paleocene hyperthermal events.

Introduction

Following the Cretaceous Tertiary boundary (65.5 Ma) Earth's climate entered a gradual warming trend during the Paleocene (65.5-55.8 Ma) reaching an optimum during the middle of the Eocene (55.8-33.9 Ma) (Bowen et. al, 2006). During this warm period, the

Earth experienced relatively short-lived, rapid, and extreme warming events referred to as hyperthermals. Numerous hyperthermal events have been identified during the Paleocene and Eocene including the Dan-C2 event, lower C29N event, Early-Late Paleocene Biotic Event, Paleocene Eocene Thermal Maximum (PETM), Elmo (ETM 2), and "X" event (ETM 3) (Ciccioni et. al, 2010) (Galeotti et. al, 2010) (Quillevere et. al, 2008) (Westerhold et. al, 2008) (Lorens et. al, 2005). Large hyperthermal events of the early Eocene are marked by negative carbon isotope excursions (CIE) in bulk carbonates and evidence of global warming from decreasing $\delta^{18}O$ values. The PETM, the most substantial hyperthermal, shows a >3‰ negative CIE in marine carbonates and decreasing carbonate $\delta^{18}O$ values which correspond to a 4 to 8°C shift in global temperature (Bowen et. al, 2006) (Pagani et. al, 2006). The rapid, and sometimes step-wise, shift in $\delta^{13}C$ values is generally followed by a more gradual recovery in carbon isotope composition over a period of 10 to 100 kyr (Galeotti et. al, 2010). Other hyperthermals, such as the Dan-C2 event, are characterized by coupled negative carbon isotope excursions (Galeotti et. al, 2010) (Quillevere et. al, 2008). Hyperthermals are also associated with decreases in the weight percentage of $CaCO_3$ signifying widespread carbonate dissolution likely due to shoaling of the lysocline (Nicolo et. al, 2007).

Consideration of all the available evidence indicates that these hyperthermals represent rapid warming caused by substantial changes in the global carbon cycle. (Pagani et. al, 2006) The negative CIEs reflect massive inputs of isotopically light carbon (such as terrestrial organic carbon, marine organic carbon, or methane hydrates) to the ocean/atmosphere reservoir. Using a range of climate sensitivity to a CO_2 doubling during the early Cenozoic, Pagani et al has found that to generate a 3‰ negative CIE

would require the addition of >5Pg of carbon from terrestrial or marine organic carbon, while only 1.5-2 Pg of carbon from methane would be required. (2006) However recent studies using high resolution datasets of the early Eocene argue the CIE must be associated with redistribution of organic carbon because the recovery after hyperthermals is too rapid for carbon input to be from sedimentary reservoirs. (Sexton et. al, 2011) The large input of new carbon into the ocean would increase acidity and decrease the carbonate saturation state, causing shoaling of the lysocline and widespread carbonate dissolution. Alternatively, some regional changes in carbonate dissolution could have been generated by changes in net primary productivity and export productivity of organic carbon and carbonate (Tappan, 1968).

Growing evidence indicates that the major hyperthermals were not isolated occurrences, but part of a continuous series of similar, but smaller events (Galeotti et. al, 2010) (Zachos et. al, 2010) (Nicolo et. al, 2007). Orbital triggers are now increasingly evident as patterns of carbonate dissolution are associated with times of increased insolation and warmer high-latitude temperatures (Galeotti et. al, 2010). Spectral analysis has been applied to detect statistically significant periodicity between hyperthermal events. Long term and short term eccentricity cycles, roughly 400kyr, 127kyr, and 96kyr, have been modeled for the early Cenezoic with high precision. (Laskar, 2004) (Palike, 2005) However tuning the data to obliquity, 41kyr, and precession cycles, roughly 23kyr and 19kyr, in the Paleocene is more imprecise due to a shorter duration of stability. (Laskar, 2004) (Palike, 2005) Numerous studies looking at the periodicity of hyperthermal events in the early Eocene have found relationships with the long and short eccentricity cycles and precession cycles. (Laurens et. al, 2005) (Galeotti et. al, 2010) (Zachos et. al, 2010)

However there are different cyclostratiographic models produce uncertainty regarding the exact timing and number of cycles between early Eocene hyperthermal events. (Laurens et. al, 2005) (Galeotti et. al, 2010)

As our understanding of these hyperthermal events progresses, it becomes clearer that small changes in orbital parameters greatly impacted the carbon cycle during this time. Regularity in carbon release appears to require a singular mechanism linked to changes in high-latitude insolation. (Galeotti et. al, 2010) Curiously, patterns of carbon release, dissolution, and warming are not pervasive during the Mesozoic, but have their onset near the K/T boundary – the time interval associated with sever global disruption resulting from an asteroid impact (Alvarez et. al, 1980). Understanding why hyperthermals, as well as the continuum of dissolution events appear to have their origins in the early Cenozoic has yet to be explored.

Previous studies have identified early Paleocene hyperthermals in the northwest Atlantic Ocean (OPD Hole 1049C) and southeast Atlantic Ocean (DSDP Holes 527 and 528), the Contessa Road Section in central Italy, and the Nile Basin in Egypt. (Coccioni et. al, 2010) (Quillevere et. al, 2008) (Bournemann, 2009) This evidence indicates that the Dan C2 event was global in scale and contain a 1‰ negative carbon isotope excursion and increased carbonate dissolution. (Coccioni et. al, 2010) This study seeks to collaborate these findings in two sections from the Tethys Sea now located in northern and central Italy; the Forada Section and the Bottaccione section. A high resolution dataset of stable isotope and carbonate disolution was developed for the early Paleocene starting at the K/T boundary in order to detect the Dan-C2 event and other minor early Paleocene

hyperthermals and to analyze the periodicity between events to better understand potential forcings of these variable climate states.

Study Location

This study contains samples from the Bottaccione section in central Italy and the Forada section in northern Italy. These outcrops were formed during the Cretaceous and Tertiary when the sediment was covered by the Tethys Sea. The limestone deposits were formed by the sedimentation of calcium carbonate shells and skeletons of marine organisms becoming lithified over millions of years.

The Bottaccione section, a >300m-thick record in Scaglia Rossa pelagic red limestone of the Umbria-Marche succession in central Italy, provides a continuous record of the upper Cretaceous and Paleocene. (Corfield et. al, 1991) This section was used to develop magneto- and biostratigraphic relationships that enabled the first calibration of geomagnetic reversals for most of the Paleogene interval (Lowrie et al., 1982). Previous studies on the Contessa Road section located just 4 km west of Bottaccione identified two major Paleocene hyperthermals; the Dan-C2 and Lower C29n event. (Coccioni et. al, 2010). My research will further develop a high-resolution isotopic record of bulk carbonates and organic carbon onwards into the Paleocene.

The Forada section is another expanded section containing a continuous record across the K/T boundary into the Paleocene. The Forada section is located the Venetian pre-Alps region of Northern Italy along Forada Creek (46.036083˚N, 12.063975˚E). The total section (62 m) is a single continuous outcropping of well exposed pelagic to hemipelagic limestones, marls, and claystones spanning the Upper Cretaceous to the lower Eocene

(Giusberti et al., 2007). The section contains the same Scaglia Rossa formation composted of rhythmically organized banding of pink-reddish limestones and marly limestones as the Contessa Road and Bottaccione sections (Giusberti et al., 2007). Forada paleodepth estimates are between 600-1000 m, and not deeper than 1500 m (Luciani et al., 2007).

Methods

Sampling

345 previously excavated samples from the Bottaccione outcrop in central Italy were used in this study. They were excavated, crushed, and stored in 5 mL plastic tubes at the Universita degli Studi di Urbino. Samples from the Forada Section were collected October 27th 2011. The K/T boundary was identified by a gray, marly, 1 cm thick layer above which lay the Scaglia Rossa formation of the early Paleocene. A 2 m section was measured out and marked for reference every 10 cm. There were a few minor delineations (1-5m horizontally) along the section where obtaining samples was difficult. The bedding plane of the outcrop was followed to obtain better samples from that same time period. Samples were collected at 2 cm intervals using a hammer and chisel to remove rock fragments from the outcrop for a total of 100 samples. Exposed surfaces were broken off so that only the interior rock fragments were placed in collection bags. The rock fragments and crushed samples from the Forada Section are housed within the Yale Geology Department, New Haven, Connecticut.

Weight Percent Calcium Carbonate

The bulk rock samples were first cleaned using a solution of DCM and methanol then crushed into a fine powder using a Retsch RS 200 rock crusher and stored in 15mL

plastic test tubes. Samples were then weighed out on a Mettler Toledo MX5 balance in 300±50μg amounts and transferred to 12 mL rounded bottomed glass test tubes sealed with a cap. Three standards comprised of pure calcium carbonate, NBS 18 (carbonatite), NBS 19 (calcite), and a Lincoln Limestone lab standard, were also weighed in amounts varying from 50-500μg to be used as references every eight samples during the runs. Test tubes were placed on a GasBench II sampling peripheral and flushed with helium. 1 mL of a 105% phosphoric acid solution, comprised of 99% phosphoric acid with 6% by weight phosphorous pentoxide, were manually added to each test tube and left to fully react for four hours. The GasBench II sampling peripheral then used helium to push the resultant carbon dioxide into the Thermal Finigan DELTA^{plus} Advantage Isotope Ratio Mass Spectrometer. The mass spectrometer was run on continuous flow mode using a CO_2 reference gas as an internal standard and measuring each sample eight times in 100μL amounts controlled by a 6-way valve. Carbonate content (weight % $CaCO_3$) was calculated using the voltage amplitude from the carbon dioxide entering the mass spectrometer, the masses of the samples, and the pressure and temperature conditions of the lab. These measurements were calibrated against the three standards of pure calcium carbonate to give weight percent calcium carbonate.

Stable Isotopes

Stable isotope measurements of both the Bottaccione and Forada samples were conducted using the same preparation on the Thermal Finigan DELTA^{plus} Advantage Isotope Ratio Mass Spectrometer with GasBench II sampling apparatus at Yale University. Oxygen isotopes for the Paleocene were ignored due to previous evidence of diagentic alteration of oxygen isotopes on the Bottaccione section. (Corfield, 1991) In addition to providing

measurements of the voltage amplitudes the mass spectrometer also measured the ratio of mass 45/44 which could be used to calculate $\delta^{13}C$. Samples were calibrated to three standards, NBS 18 ($\delta^{13}C$= -5.01‰), NBS 19 ($\delta^{13}C$= 1.95‰), and a lab standard of unknown $\delta^{13}C$, which were sampled at the beginning and end of each run and every eight samples in between. All of the stable isotope measurements are reported in per mil (‰) relative to the VPDB standard.

The weight percent calcium carbonate and $\delta^{13}C$ measurements were conducted over 14 runs on the GasBench containing 54 to 70 samples and 18 standards per run. The DeltaPlus XP mass spectrometer had a failure in an electonics motherboard after the first run and the replacement part was backordered for several months, so measurements were switched to the DeltaPlus Advantage for all subsequent runs. The DeltaPlus Advantage mass spectrometer was capable of making carbonate measurements but had not previously been used to measure $\delta^{13}C$ of carbonates.

In total 1,071 samples and standards were weighed out and reacted on the GasBench. Runs 2, 3, 4, and 11 were not included in the dataset because they did not produce enough reliable standards to calibrate from or experienced extended time delays preventing accurate measurements accounting for 287 of the failed samples and standards. Within the other successful runs 183 of the samples and standards had to be rerun due to too low of voltage amplitudes, not the expected number of voltage peaks, air contamination, or other inconsistencies with the measurements. 345 samples from Bottaccione, 100 samples from Forada and 156 standards were included in the final dataset.

Results

Data Analysis

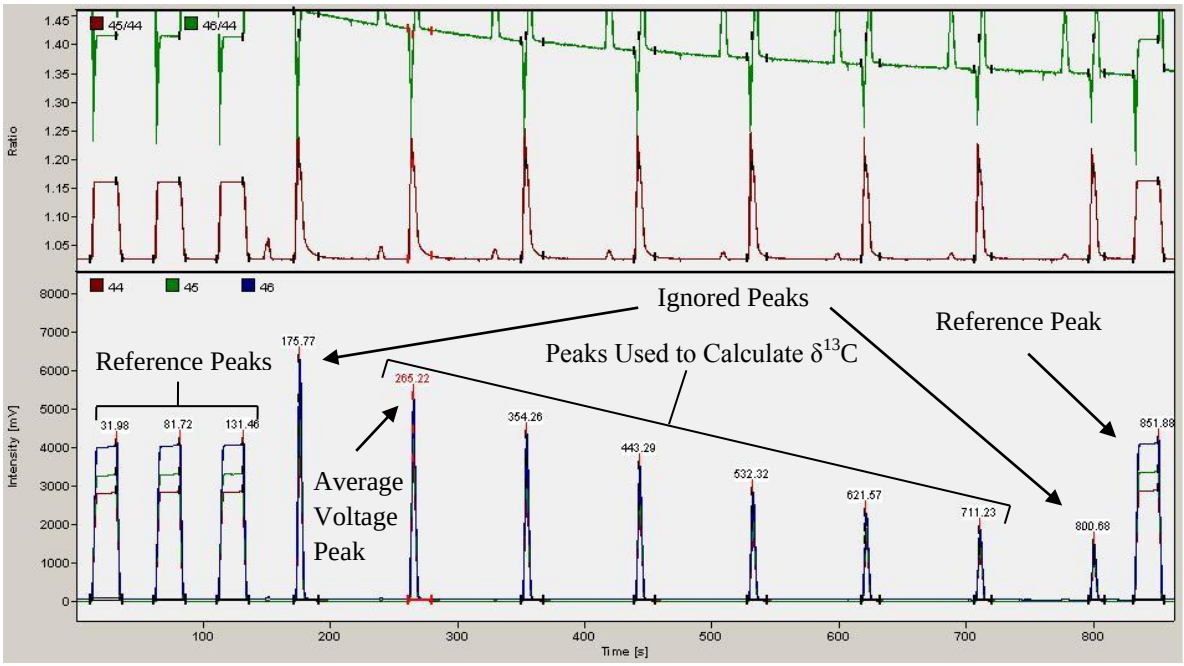

Figure 1 Raw Data From Mass Spectrometer for Lab Standard B 200 in Run 6

Measurements from the Thermal Finigan DELTA^{plus} Advantage Isotope Ratio Mass Spectrometer were interpreted using the IsoDat Workspace software program. Each sample or standard produced a time series of voltages during the continuous flow mode for different masses with twelve peaks as depicted in Figure 1. Each measurement began with three voltage peaks corresponding to the reference gas, followed by eight voltage peaks corresponding to the values for masses 44, 45, and 46 within the CO_2 gas produced from the sample, followed by one final reference gas peak. Comparing the ratios of these masses provides the $\delta^{13}C$ values using the equation:

$$\delta^{13}C = [(^{13}C/^{12}C_{Sample}) / (^{13}C/^{12}C_{PDB}) - 1] * 1000$$

For this equation mass 44 represents ^{12}C, and mass 45 represents ^{13}C. Mass 45 is also affected by ^{17}O within the CO_2 however we assume that when calibrating the sample to

the known $\delta^{13}C$ value for the standards this correction factor will accounts for inputs from ^{17}O along with variability between instruments and runs. To calculate the average measured $\delta^{13}C$ value for the sample or standard the first and last of the eight peaks were ignored to prevent outliers and the linear intercept of the middle six peaks (plotted against their order) was used as the average $\delta^{13}C$ value. This decay is due to the isotope signal decaying slightly as less CO_2 is pushed through the mass spectrometer. The amplitude of the voltage of the second non reference gas peak was used as the average voltage for the entire sample or standard. 183 of the 445 samples had to be remeasured due to too low of voltages to produce accurate $\delta^{13}C$ measurements, or producing extra or not enough peaks during their initial runs.

Weight Percent Calcium Carbonate

Weight percentage of calcium carbonate was calculated by first developing a linear regression, with an intercept of 0, of the masses of the standard versus the voltage amplitude produced by each of the standards within the run. This regression provides a value representing 100% weight percent calcium carbonate which varies for each run as shown in Table 1 and Figure 2. Weight percent calcium carbonate can then be calculated by the following equation:

Weight % $CaCO_3$ = [(Amplitude of Sample) / (Regression Slope*Mass of Sample)]*100

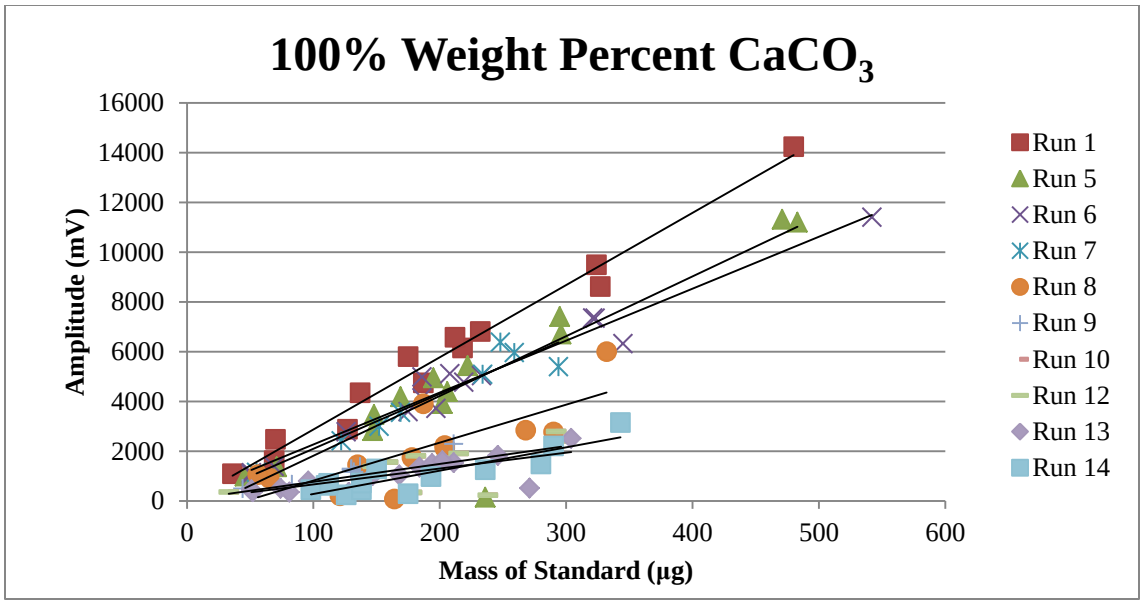

Figure 2 Regression Lines for Weight % $CaCO_3$ of Standards

After the values for $\delta^{13}C$ were calculated they must also be calibrated for each individual run using the standards. To calibrate the samples this study used two corrections; a drift correction and an amplitude correction. First the know values for NBS 18 and NBS 19 (-5.014‰ and 1.95‰ respectively) were subtracted from the measured $\delta^{13}C$ values for each standard to produce a difference from standard value.

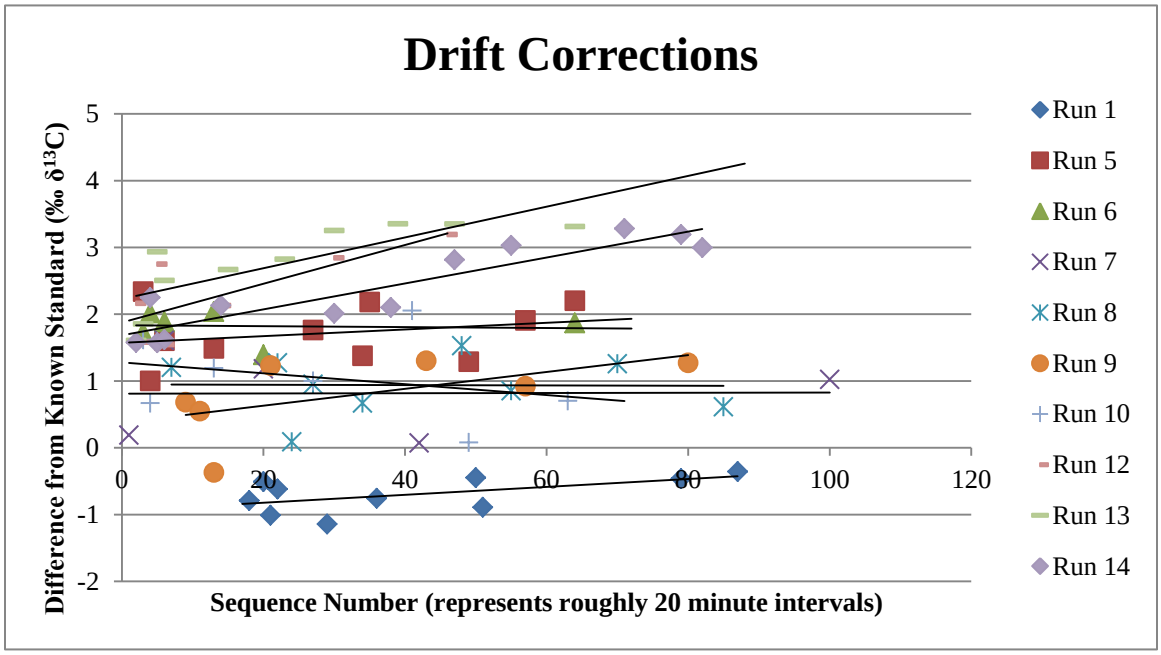

Figure 3 Linear regressions for Drift Corrections using difference from known standard against time intervals given by the sequence number adjust for delays

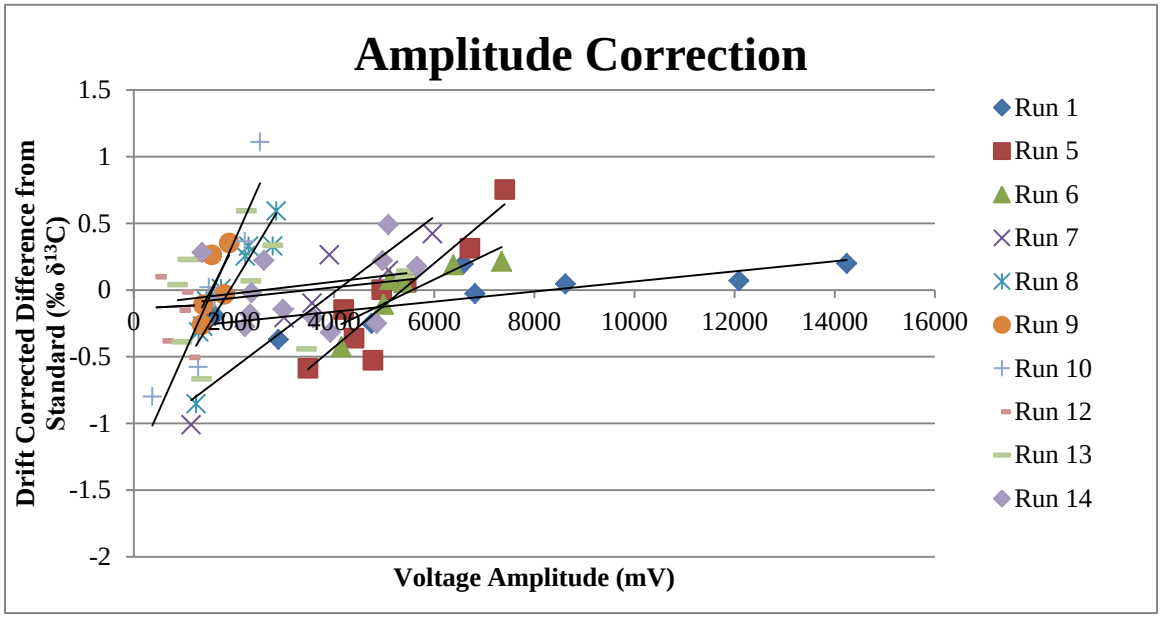

Figure 4 Linear regressions for Amplitude Corrections using drift corrected difference from known standard against voltage amplitude

The drift correction was used to account for the minor changes in $\delta^{13}C$ over the length of the run. The sequence number of the sample within a run (adjusted to account for delays during the run) can be used to denote the time between sampling. $\delta^{13}C$ difference from the known value of each standard was plotted against sequence number to develop a linear regression for the drift correction for each run as shown in Table 1 and Figure 3. Outliers exceeding ±1‰ of the mean value of each run were removed when developing the linear regression and the total number of standard used is also listed in Table 1.

The amplitude correction was used to account for the minor increase in $\delta^{13}C$ as the voltage amplitude increases. After the drift correction was applied, $\delta^{13}C$ difference from the known value of each standard was plotted against voltage amplitude to develop a linear regression for the amplitude correction for each run as shown in Table 1. Outliers exceeding ±1‰ of the mean value of each run were removed to calculate the regression for the amplitude correction and the total number of standards used per run is given in

Table 1. Corrected $\delta^{13}C$ could then be calculated for each sample using the following equation with the correction factors for each run in Table 1:

Corrected $\delta^{13}C$ = Original $\delta^{13}C$ – ((DS*Sequence Number)-DI) – ((AS*Amplitude)-AI)

Weight % $CaCO_3$				**$\delta^{13}C$ Corrections**						
Run	Slope	R^2	#	Drift Slope (DS)	Drift Intercept (DI)	R^2	Amp Slope (AS)	Amp Intercept (AI)	R^2	#
Run 1	28.91	0.98	13	0.005936	-0.94	0.32	0.000032	-0.25	0.62	8
Run 5	23.30	0.98	14	0.004998	1.57	0.07	0.000315	-1.69	0.85	8
Run 6	22.93	0.96	13	-0.000658	1.83	0.00	0.000181	-1.00	0.74	6
Run 7	21.39	0.98	9	-0.009040	1.53	0.29	0.000283	-1.15	0.87	5
Run 8	10.07	0.97	14	-0.000259	0.95	0.00	0.000620	-1.19	0.80	9
Run 9	8.79	0.91	10	0.007220	0.73	0.39	0.000724	-1.12	0.47	5
Run 10	7.78	0.97	10	-0.008176	1.28	0.09	0.000846	-1.33	0.87	6
Run 12	5.20	0.88	6	0.028998	1.88	0.58	0.000020	-0.14	0.00	6
Run 13	10.03	0.88	11	0.023047	2.23	0.62	0.000044	-0.12	0.04	10
Run 14	12.35	0.85	14	0.019405	1.68	0.83	0.000040	-0.14	0.04	12

Table 1 Linear Regressions for Weight % and $\delta^{13}C$ Correction Factors

Uncertainty

Uncertainty within the stable isotope measurements was calculated by applying the drift and amplitude corrections to the lab standard. The lab standard was not used in developing the correction factors but if the corrections were properly applied should result in a single value and therefore can be used to test the accuracy of the correction factors. When the correction factors were applied to the lab standard and outliers were removed they resulted in a mean value of 0.90‰ $\delta^{13}C$ with each run producing different variability as outlined in Figure 5. The standard deviation between all the corrected lab standards with outliers removed was 0.32 representing ±0.32‰ $\delta^{13}C$ of uncertainty for

each of the samples. However using the full dataset with outliers included the uncertainty increases to ±2.22‰ $\delta^{13}C$.

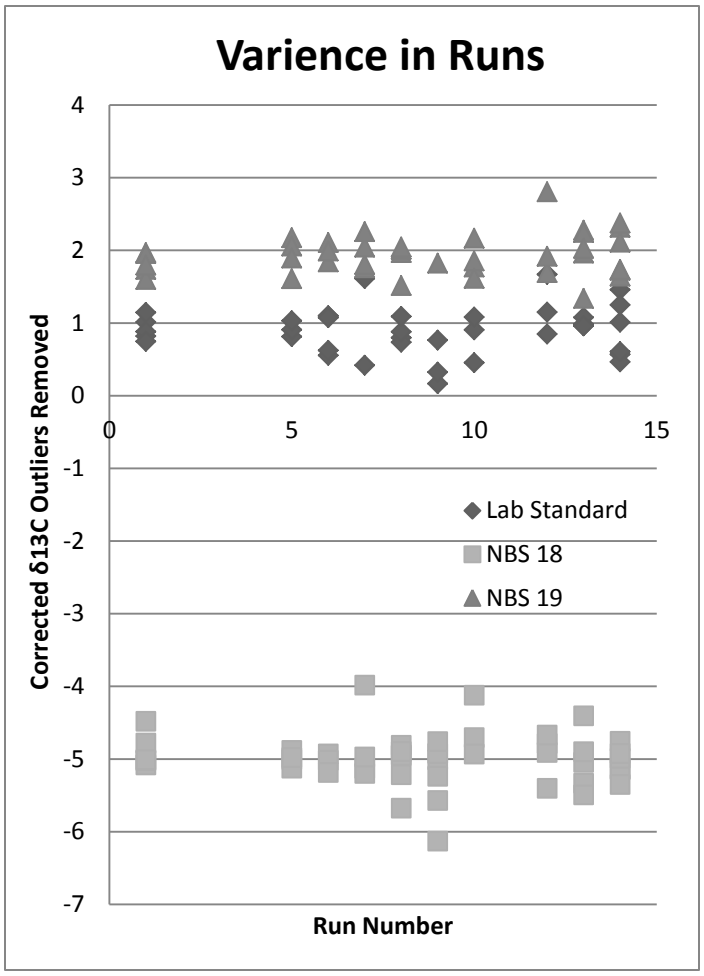

Figure 5 Corrected $\delta^{13}C$ for standards across runs

In addition to applying the corrections to the lab standards the corrections were also applied to the standards NBS 18 and NBS 19 used to derive the equations. Most all of the linear regressions for drift correction and amplitude correction had R^2 values much lower than 0.90 indicating weak correlations. Due to this variability within the measurement of these know standards NBS 18 and NBS 19 also showed standard deviations of ±0.36‰ $\delta^{13}C$ and ±0.28‰ $\delta^{13}C$ respectively. However the corrections were successful in shifting the mean values of the standards to the know isotope values and decreasing the standard deviation of both NBS 18 and NBS 19.

Carbonate dissolution measurement calculated from the weight percent calcium carbonate had even greater uncertainty. The linear regressions calculating 100% $CaCO_3$ from the three standards of either pure calcite or limestone had high R^2 values for each run indicating a strong correlation between weight and the amplitude of voltage. However when these corrections were applied to each standard they produced a wide range of weight percent calcium carbonate values. After removing outliers, the standard

deviation for weight percent calcium carbonate for the lab standard, NBS 18, and NBS 19 was ±16.5%, ±16.8%, and ±17.1% respectively.

Discussion

The data analysis this study performed on the stable isotope and carbonate dissolution measurements is a standard methodology used throughout the literature. The Isodat Workspace is a commonly used software package to evaluate the voltage amplitudes and determine $^{13}C/^{12}C$ ratios. Previous studies also employ set of standards to be sampled throughout the run to help calibrate the results based on their drift and amplitude. NBS 19 is a preferred standard when working with limestone samples because it comes from a single slab of white marble as opposed to NBS 18 which contains $CaCO_3$ in the form of calcite from a carbonatite rock. (Friedman, O'Neil, & Cebula, 1982) The lab standard was also prepared from a single homogenous source, "lincoln limestone", that contained $\delta^{13}C$ values similar to NBS 19 and the limestone sampled. While the drift and amplitude corrections failed to lower the standard deviation of the dataset to a statistically significant level they were successful in calibrating the standards to know values and decreasing the variance in the data. Figure 6 shows the standard deviation in the lab standard $\delta^{13}C$ values for the original data, the corrected

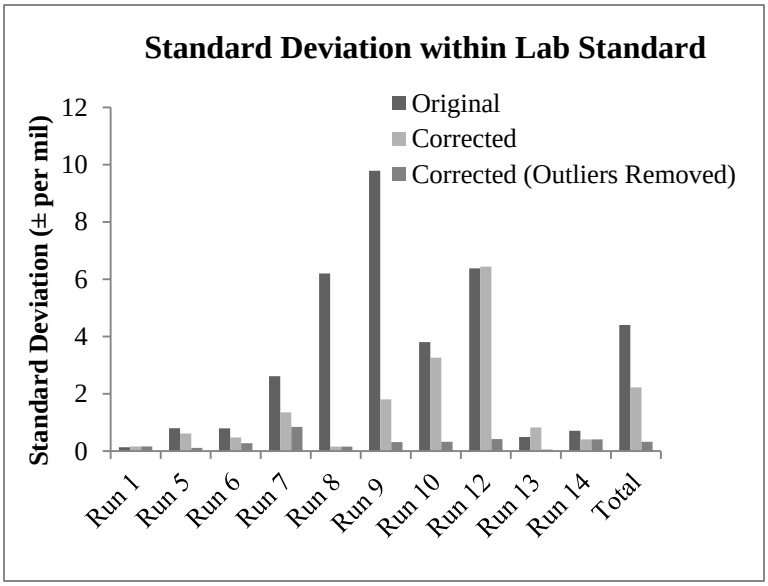

Figure 6 Standard Deviation across Runs

data, and the corrected data removing outliers for each run. This graph indicates a clear trend of the corrections improving the variance but reaching an upper limit established by the precision of the mass spectrometer. After corrections and removing outliers this upper limit on the variance throughout all of the runs appears to be roughly ±0.10‰ with an average value, established by the total variance within the lab standards, of ±0.32‰.

The methodology used in measuring carbonate dissolution is not the standard used throughout the literature but still an acceptable method for calculating weight percent $CaCO_3$. Other studies have used a Dietrich-Fruhling calcimeter which utilizes the same techniques as performed on the GasBench; dissolving pre-weighted samples in a phosphoric acid solution and factoring in temperature and pressure to compare the volume of CO_2 gas produced to the mass of sample. (Galeotti et al, 2010) (Coccione et. al, 2010) The Dietrich-Fruhling calcimeter can measure larger masses of samples (around 300mg as opposed to 300μg) and has a precision of roughly ±1%. (Galeotti et al, 2010) Evaluating based on the variance in the weight percent $CaCO_3$ of the lab standards this study had a precision of ±16.5%. The calcimeter's ability to process larger amounts of a sample provides a more robust calculation from the CO_2 produced. While this study contained a larger uncertainty than using the calcimeter I argue that the methodology is not inherently more imprecise but errors with the mass spectrometer, as also indicated with the high variance in stable isotope measurements, generated most of the uncertainty.

One possible source of error is from a memory effect generated by the lab equipment. A memory effect occurs when an instrument allows for one sample to contamination the following sample by not fully removing that sample before the next one enters. If a memory effect were to occur it would most likely occur in the 100µL loop between the 6-way valve that loads the CO_2 gas from the GasBench into the mass spectrometer. This dataset was checked for evidence of a memory effect by plotting the uncorrected $\delta^{13}C$ values and comparing those samples that occurred after an NBS 18 standard to the rest of the data. NBS 18 has a much more negative value of -5.014‰ which if there was a memory effect one would expect the measurements following an NBS 18 standard to be slightly more negative than the other values. Figure 7 illustrates that samples following the NBS 18 standard contained the same distribution as other Bottaccione samples. I argue that a memory effect was not evident in this data and that other sources of error were the causes for uncertainty in the data set.

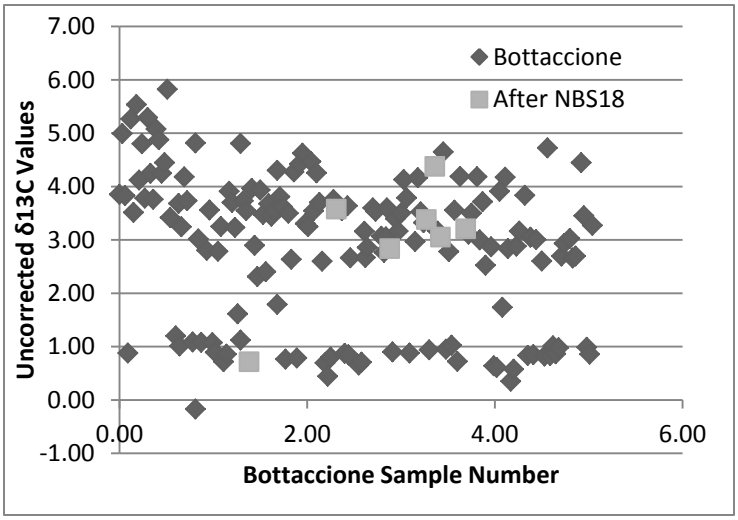

Figure 7 Uncorrected $\delta^{13}C$ values from Bottaccione samples comparing samples run after NBS 18 to the rest of the data

Another way to explain the uncertainty within the data is to look at the outliers that were removed and try to find correlations that may explain sources of error. Of the 156 standard used in this analysis 43 were determined to be outliers. 20 standards contained $\delta^{13}C$ values in excess of ±1‰ of the run's mean, 16 standards contained weight % $CaCO_3$ less than 60%, and 7 contained errors with both measurements. The observation that 28%

of the standards in this dataset can be evaluated as outliers is a clear indication of the high levels of uncertainty in these measurements.

The voltage amplitude is one important factor in analyzing the outliers. A final run of just 30 standards measured out at different masses from 0 to 500μg was performed to estimate the lower limits of the mass spectrometer's ability to evaluate $\delta^{13}C$ at a given voltage. This run demonstrated that below roughly 500mV the data was most unreliable. Figure 8 illustrates the standard deviation within the samples at 500V intervals and shows that the lowest amplitudes have a significantly higher variance than the higher voltages. Of the 7 samples producing outlier values for both $\delta^{13}C$ and weight % $CaCO_3$ all of them had amplitudes lower than 500mV.

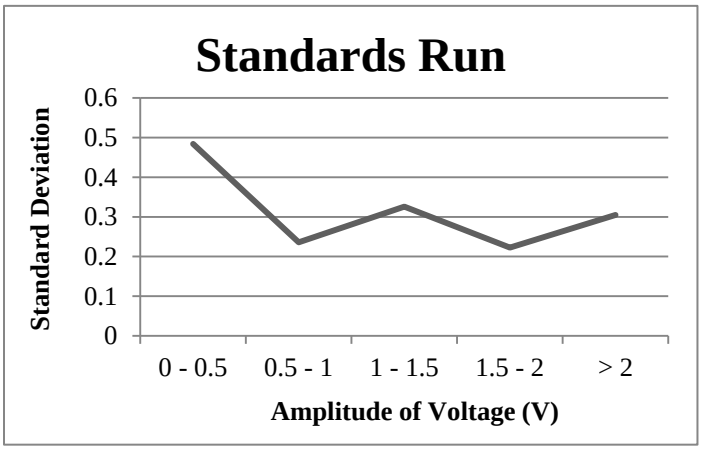

Figure 8 Standard deviation across voltage ranges

Extremely high voltages have also been found to be a source of error and skew the $\delta^{13}C$ correction. In this dataset a few standards produced voltage amplitudes upwards of 10,000mV which did not always correlate to the linear regressions calculated using primarily lower voltages. Therefore when these corrections were applied to the higher voltages they resulted in $\delta^{13}C$ values that were lower due to the amplification of this negative amplitude correction.

A third source of error within the outliers was from time delays within the measurements. Most runs occurred continuously over a period of roughly 18 hours however some runs

such as run 7 and run 13 had mechanical issues with the GasBench where the sampling needle was misaligned and had to be readjusted causing a discontinuous sampling. The dataset attempted to account for this by adjusting the sequence number of the standard in the later half to the time lag but this failed to resolve the issue. This signifies that the changes in $\delta^{13}C$ over the length of the run due to drift is not a result of the time the standards have reacted but more likely a factor related to continuous sampling on the mass spectrometer. Using low voltage, high voltage, and time delays to explain the outliers accounts for roughly half of the outlier values. However there are still 10 outliers for weight % $CaCO_3$ and 14 outliers for $\delta^{13}C$ that remain unaccounted for.

Using the corrections applied to the $\delta^{13}C$ values for the lab standard and removing any outliers exceeding ±1‰ of the mean $\delta^{13}C$ value of each run, the uncertainty of the dataset was determined to be ±0.32‰. However due to the fact that only half of the outliers could be explained those unaccounted for outliers should be included which increases the standard deviation to ±0.39‰. For carbonate dissolution measurements removing any weight % $CaCO_3$ values less than 50% for the lab standard result in an uncertainty of ±16.5%. However including unaccounted for outliers would produce a more realistic uncertainty of ±20.2%.

Source of error could also have occurred throughout the measurement process that cannot be easily confirmed through the given measurements. Contamination issues are one likely possibility. Samples and standards could have been contaminated by the spoon used to weigh samples, the weighing trays, the glass test tubes, the H_3PO_4 acid solution, or the air. Precautions were taken to wipe down the weighing spoon between samples and to only use cleaned weighing trays and test tubes that were unexposed to the air, however

contamination could have still occurred. The phosphoric acid solution may have contain trace amounts of water whose oxygen atoms could have reacted with the sample and left a small signal from the ^{17}O isotopes affecting $\delta^{13}C$ calculations. However, the phosphoric acid solution contained 6% by weight phosphrous pentoxide which is used to help evaporate any trace amounts of water that may be present within the acid so acid contamination is unlikely to be a possibility. Air contamination is a stronger possibility due to the fact that small voltage peaks were observed just before the CO_2 voltage peaks in many samples. These peaks pertain to small amounts of nitrates containing mass 44 and mass 45 that were separated out during the gas chromatography phase of the mass spectrometer. This air could have also contained CO_2 not derived from the reaction between the acid and the sample thus impacting the $\delta^{13}C$ values. Figure 9 illustrates these air peaks observed in numerous samples and standards.

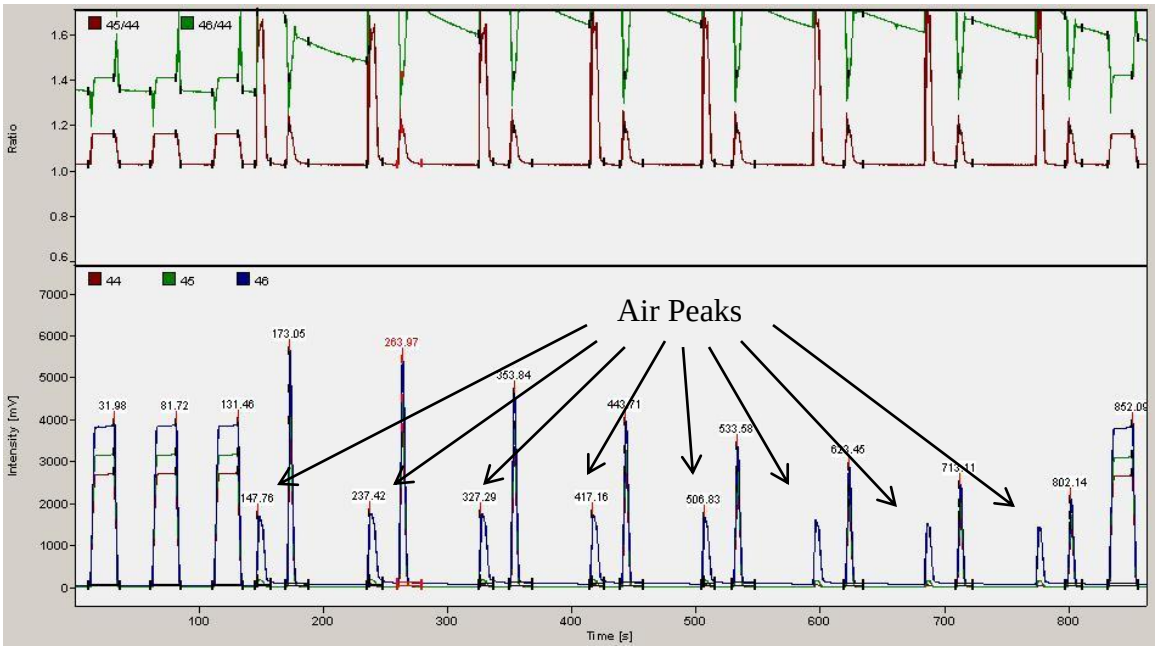

Figure 9 Air peaks from nitrates observed in NBS 18 A 200 from run 7

A final contamination factor that must be considered is that the standards themselves were contaminated. Contamination of the standard containers could have occurred as Ithe

	Weight Percent $CaCO_3$		$\delta^{13}C$ Values		
Standard	All Standards	Outliers Removed	Original Values	Corrected Values	Corrected Values Outliers Removed
Lab Standard	±31.5%	±16.5%	±4.40‰	±2.22‰	±0.32‰
NBS 18	±26.3%	±16.8%	±1.72‰	±1.13‰	±0.36‰
NBS 19	±28.7%	±17.1%	±2.95‰	±1.09‰	±0.28‰

Table 2 Total standard deviation of each standard throughout the dataset

standards were weighed out or from previous experiments. However this is unlikely due to the fact that three separate standards were used throughout the experiment and each of them experienced similar levels of variance as shown by Table 2. For contamination of the standard to be the source all three of the standards must have experienced the same level of contamination which could have occurred despite precautions to clean the weighing spoon between samples and keeping the standards unexposed to the air.

Beyond contamination of samples another source of error may stem from the reaction of the sample with the acid. Rounded bottom test tubes were used to ensure that all of the sample and the acid settled to the bottom of the test tube however when transferring the sample from the weighing tray to the test tube some of the sample may have not reached the bottom of the tube. Likewise the phosphoric acid was highly viscous and tended to cling to the edges of the test tube and may have not fully reached the standard at the bottom of the test. However it is very likely that most of the sample and acid remained in the bottom of the test tube to react.

Reaction temperature also was not properly maintained throughout the experiment. Typically the GasBench automatically adds acid to each sample at defined intervals but this experiment added acid manually due to errors with the sampling needle. Acid was added in test tube racks at the lab temperature of 22°C while the GasBench is typically

heated to a temperature of 26°C. Each run was left to fully react for at least four hours but was transferred from the 22°C to the 26°C environment at different times. These temperature differences could potentially have an effect on the equilibration of how much CO_2 produced remains dissolved within the acid and how much is released as a gas to be sampled by the mass spectrometer. A study by Torres, Mix, and Rugh in 2005 found that temperature can significantly affect the dissolution of CO_2 when measuring dissolved inorganic carbon of seawater using the GasBench sampling apparatus. When they chilled samples during equilibration at a controlled temperature of 12°C they found an improvement in the precision of the $\delta^{13}C$ measurements from ±0.15‰ to ±0.11‰. (Torres, Mix, & Rugh, 2005) Other studies on carbonate samples suggest performing the reactions in a vacuum at a controlled temperature of 90°C can improve the precision of the $\delta^{13}C$ measurements to ±0.05‰. (Velivetskaya, T., Ignatiev, A., & Gorbarenko, S., 2009) While the temperature differences may be much smaller at 4°C impacts on the equilibration of CO_2 gas in the test tube would have significant consequences on the amount of sample entering the mass spectrometer. This is one mechanism to explain the large amount of samples with low voltage amplitudes.

Previous studies have found that during the Paleocene and Eocene natural background $\delta^{13}C$ variability is less than 0.2‰. (Corfield et al., 1991) Hyperthermal events are marked by negative carbon isotope excursions (CIE) typically on the order of magnitude of roughly 1-2‰ with the largest hyperthermal, the Paleocene-Eocene Thermal Maximum, containing a 2-3‰ CIE. (Zachos et. al, 2005) Early Paleocene hyperthermals including the Dan-C2 event were on the order of magnitude of a 1‰ negative CIE. (Coccioni et. al, 2010) Therefore when the ±0.39‰ uncertainty of the dataset is placed overtop the ±0.1‰

natural variability the result is a ±0.49‰ variability within the background values making a 1‰ negative CIE extremely difficult to accurately quantify.

Greater uncertainty lies when using the carbonate dissolution data from these measurements. Evidence from past studies from the Tethys Sea suggest that during the majority of the early Cenezoic the carbonate saturation state lay deep within the sea causing the weight percent calcium carbonate of the limestone to range from 90-100% likely varying due to net primary productivity. (Galleotti et. al, 2010) However during hyperthermal events evidence suggests that inputs of carbonate to the system caused the calcium compensation depth to rise leading to widespread carbonate dissolution in sediments. Previous studies have found that during hyperthermal events weight percent $CaCO_3$ decreased to upward of 60%. (Galleotti et. al, 2010) This study found an uncertainty of ±20.2‰ for weight percent $CaCO_3$ which imposed overtop the 10% natural variability could account for a majority of the carbonate dissolution that may be caused by hyperthermal event.

Conclusions

Due to the uncertainty within the dataset correction factors were not applied to the samples in order to identify early Paleocene hyperthermal events in the Tethys Sea and analyze the periodicity between events. This study found that minimizing uncertainty within measurement is critical in being able to evaluate hyperthermal events. This analysis maintains that the methodologies used in this experiment could produce statistically significant data but the GasBench II sampling periphery and DeltaPlus Advantage mass spectrometer contained errors causing imprecise measurements.

However this study would recommend using a Dietrich-Fruhling calcimeter to measure carbonate dissolution due to its ability to process large masses and produce much less uncertainty. Evaluating outlier data this study found that uncertainty in $\delta^{13}C$ increase when the voltage amplitude become less than 500mV and the correction factors do not pertain well to samples with voltages higher than 10,000mV or sample occurring after longer time delays during a run. In order to develop statistically significant data to evaluate the Paleocene hyperthermals uncertainty within the measurements should be on the order of ±0.05‰ $\delta^{13}C$ and ±2% weight percent $CaCO_3$. Instead the dataset from this study contain uncertainties of ±0.32‰ $\delta^{13}C$ and ±16.5% weight percent $CaCO_3$. This level of uncertainty would not be able to capture the background natural variability or accurately detect negative carbon isotope excursions and carbonate dissolution occurring during the hyperthermals. Further study on hyperthermal events during the early Paleocene is necessary to better understand the evolution of these events after the K/T boundary and the changes in orbital parameter likely to trigger such rapid warming events.

Acknowledgements

I would like to thank Mark Pagani, Simone Galeotti, and Domini Colosi for helping advise me through developing this research, collecting samples, and measuring the data. I would also like to thank the Yale Geology Department, Università degli Studi di Urbino, Yale Science and Engineering Association, and Mellon Forum Fellowships for helping provide funding to travel to Italy and collect samples for this research.

References

Alvarez, L. et al. 1980. *Extraterrestrial cause for the Cretaceous-Tertiary extinction*. Science. 1095-1108.

Bornemann, A. et al. 2009. *Latest Danian carbon isotope anomaly and associated environmental change in the southern Tethys (Nile Basin, Egypt).* Journal of the Geological Society, London. 1135-1142.

Bowen, G. et al. 2006. *Eocene hyperthermal event offers insight into greenhouse warming.* Transactions of the American Geophysical Union. 165-169.

Coccione, R. et al. 2010. *The Dan-C2 hyperthermal event at Gubbio (Italy): Global implication environmental effects and cause(s).* Earth and Planetary Science Letters. 1-8.

Corfield, R., Cartlidge, J., Premoli-Silva, I., & Housley, R. 1991. *Oxygen and carbon isotope stratigraphy of the Palaeogene and Cretaceous limestones in the Bottaccione Gorge and the Contessa Highway sections, Umbria, Italy*. Terra Nova. 414-422.

Friedman, I., O'Neil, J., & Cebula, G. 1982. *Two new carbonate stable isotope standards*. Geostandards Newsletter. 11-12

Galeotti, A. et al. 2000. *Integrated stratigraphy across the Paleocene/Eocene boundary in the Contessa Road section, Gubbio (central Italy)*. Bulletin de la Societe Geologique de France. 355-365.

Galeotta, S. et al. 2010. *Orbital chronology of early Eocene Hyperthermals from the Contessa Road section, central Italy*. Earth and Planetary Science Letters. 192-200.

Giusberti, L. et al. 2007. *Mode and tempo of the Paleocene-Eocene thermal maximum in an expanded section from the Venetian pre-Alps*. Geological Society of America Bulletin. 391-412.

Herbert, T., & Fischer, A. 1986. *Milankovitch climatic origin of mid-Cretaceous black shale rhythms in central Italy.* Nature. 739-743.

Laskar, J. et al. 2004. *A long-term numerical solution for the insolation quantities of the Earth*. Astronomy and Astrophysics. 261-285.

Laurens, L. et al. 2005. *Astronomical pacing of the late Paleocene to early Eocene global warming events.* Nature. 1083-1087.

Lowrie, W. et al. 1982. *Paleogene magnetic stratigraphy in Umbrian pelagic carbonate rocks: The Contessa sections, Gubbio.* Geological Society of America Bulletin. 413-432.

Luciani, V. et al. 2007. *The Paleocene-Eocene thermal maximum as recorded by tethyan planktonic foraminifera in the Forada section (northern Italy)*. Marine Micropaleontology. 189-214.

Nicolo, M. et al. 2007. *Multiple early Eocene hyperthermals: Their sedimentary expression on the New Zealand continental margin and the deep sea.* Geological Society of America. 699-702.

Pagani, M. et al. 2006. *An ancient carbon mystery*. Science. 1556-1557.

Pälike, H. 2005. *Orbital variation (Including Milankovitch cycles)*. Elsevier Ltd. 410-421

Pälike, H. 2006. *Incorporation of geologic cycles in establishing geological timescales.* Paleontological Society Short Course, Exercise Notes. 1-30.

Quillevere, F. et al. 2008. *Transient ocean warming and shifts in the carbon reservoirs during the early Danian.* Earth and Planetary Science Letters. 600-615.

Sexton, P. et al. 2011. *Eocene global warming events driven by ventilation of oceanic dissolved organic carbon*. Nature. 349-353.

Tappan, H. et al. 1968. *Primary production, isotopes, extinctions and the atmosphere.* Palaergeography, Palaeoclimatology, Palaeoecology. 377-403.

Torres, M., Mix, A., & Rugh, W. 2005. *Precise delta C-13 analysis of dissolved inorganic carbon in natural waters using automated headspace sampling and continuous-flow mass spectrometry*. Limnology and Oceanography Methods. 349-360.

Velivetskaya, T., Ignatiev, A., & Gorbarenko, S. 2009. *Carbon and oxygen isotope microanalysis of carbonate*. Rapid Communications in Mass Spectrometry. 2391-2397.

Zachos, J. et al. 2005. *Rapid acidification of the ocean during the Paleocene-Eocene Thermal Maximum.* Science. 1611-1615.

Zachos, J. et al. 2010. *Tempo and scale of late Paleocene and early Eocene carbon isotope cycles: Implications for the origin of hyperthermals*. Earth and Planetary Science Letters. 242-249.